Coordination Chemistry Reviews 252 (2008) 2540–2551

Contents lists available at ScienceDirect

Coordination Chemistry Reviews

journal homepage: www.elsevier.com/locate/ccr

Review

Energy migration within the ^2E state of Cr^{3+}

Mia Milos, Sélim Kairouani, Sébastien Rabaste, Andreas Hauser*

Département de Chimie Physique, Université de Genève, 30 quai Ernest-Ansermet, CH-1211 Genève 4, Switzerland

Contents

ARTICLE INFO

Article history:
Received 17 January 2008
Accepted 14 April 2008
Available online 22 April 2008

Keywords:
Resonant and phonon-assisted excitation energy migration
$[Cr(ox)_3]^{3-}$
Fluorescence line narrowing
Spectral diffusion

ABSTRACT

Excitation energy migration is an important phenomenon at high concentration of luminescent chromophores. In crystalline solids it results in a quenching of the intrinsic luminescence of the chromophore as the excitation energy migrates to impurity centres or other forms of trap sites. As concluded from the extensively studied systems where Cr^{3+} is doped as the active chromophore into inert host lattices, energy migration in crystalline solids is usually a phonon-assisted process, in which the simultaneous creation or annihilation of phonons helps to bridge the energy miss-match in the energy levels of two neighbouring chromophores within a inhomogeneously broadened absorption band. However, in the three-dimensional network systems $[Ru(bpy)_3][NaCr(ox)_3]$ and $[Rh(bpy)_3][NaCr(ox)_3]ClO_4$, it proved possible to unambiguously identify three different mechanisms for energy migration within the R_1 line of the $^4A_2 \rightarrow {}^2E$ transition of Cr^{3+}. In addition to the common temperature dependant phonon-assisted process, a resonant process between the zero-field split components of the $^4A_2$ ground state leading to a multi-line pattern in a fluorescence line narrowing spectrum and a quasi-resonant process within the same component leading to fast spectral diffusion can be identified at very low temperature. The parameters governing these processes are discussed and the behaviour of the model systems is compared to more conventional doped oxides and related systems.

1. Introduction

Excitation energy transfer processes are subject of continuing attention since they play an important role in many areas of physics, chemistry and biology. In such a process, the excitation energy is transferred from an initially excited chromophore, the donor, to a nearby chromophore, the acceptor. Excitation energy transfer processes are important for solid state lasers [1], fluorescent lamps and displays [2], solar energy conversion cells [3], conformational analyses of proteins and investigations on the folding dynamics of DNA [4], and many other areas of current research. For high chromophore concentrations, the excitation energy can be transferred over longer distances in a sequence of transfer steps in which donor and acceptor are chemically identical and in which the acceptor

* Corresponding author. Tel.: +41 22 379 6559; fax: +41 22 379 6103.
E-mail address: andreas.hauser@unige.ch (A. Hauser).

0010-8545/$ – see front matter © 2008 Elsevier B.V. All rights reserved.
doi:10.1016/j.ccr.2008.04.006

in one step becomes the donor for the next step. This is generally referred to as energy migration [5].

Excitation energy can be transferred from the initially excited donor to an acceptor via radiative and non-radiative processes [6]. Radiative energy transfer is a sequential process in which the donor emits a photon, which, in turn, is reabsorbed by the acceptor. The probability of a radiative energy transfer process is proportional to the concentration of the acceptor, the spectral overlap integral between the emission of the donor and the absorption of the acceptor, and it depends on the shape and size of the sample, but it does not require any explicit interaction between donor and acceptor and is therefore of long-range nature. Radiative processes may become important in large samples such as laser crystals. With regard to energy migration, they result in an apparent increase of the observed luminescence lifetime, a phenomenon referred to as photon trapping [7]. For instance, the observed lifetime of the $^2F_{5/2} \rightarrow {}^2F_{7/2}$ emission in YAG:Yb^{3+} increases from the intrinsic value of 0.95 ms in a diluted and optically thin sample to around 1.3 ms for larger crystals [8]. Likewise, in Al_2O_3:Cr^{3+} (ruby) the apparent lifetime of the R-line emission may increase from the intrinsic value of 3.8 ms up to 12 ms [7].

In a non-radiative energy transfer process, the deactivation of the donor and the excitation of the acceptor take place simultaneously and thus requires an electronic interaction between the two. In 1948, Förster [9] proposed the first mechanism for non-radiative energy transfer based on electric-dipole–electric-dipole interaction between the donor and the acceptor transition dipole moments of the respective excitations. As dipole–dipole interactions fall off as R^{-3}, they are of comparatively long-range nature. Dexter [10] extended the work of Förster to include higher order multipole interactions and magnetic dipole interactions as well as exchange interactions. The latter may become dominant if the two chromophores are in close contact with each other, for instance, two metal centres via a common bridging ligand or organic chromophores via $\pi\pi$-stacking. If such is the case, super-exchange may substantially enhance the interaction at short distances, and if sufficiently strong, the energy transfer may occur as excitonic motion [11] rather than as simple hopping. Both mechanisms consider the energy transfer to be a resonant process, that is, the energy provided by the donor is entirely transferred to the acceptor. Thus, the absorption of the acceptor transition must energetically match the emission of the donor transition. If such is not the case, an eventual energy mismatch can be bridged by the creation or annihilation of vibrational energy in a so-called phonon-assisted process [12]. Phonon-assisted energy transfer and energy migration is a common phenomenon in systems having narrow absorption and emission lines with generally small or no spectral overlap such as f–f transitions in lanthanide containing systems or spin–flip transitions in transition metal ions [13]. Phonon-assisted energy transfer is strongly temperature dependent and usually freezes in at low temperatures.

One of the model systems for studying energy migration in inorganic solids is provided by the spin-forbidden $^4A_2 \rightarrow {}^2E$ transition of Cr^{3+} [14] in octahedral coordination in a moderate to strong ligand field. In Section 2, the relevant physical parameters are discussed and the corresponding literature is briefly reviewed. In Section 3, the theoretical concepts for excitation energy transfer, with emphasis on energy migration at high chromophore concentration, are introduced. As discussed in detail in Section 4, the three-dimensional oxalate networks of compositions $[Ru(bpy)_3][NaCr(ox)_3]$ and $[Rh(bpy)_3][NaCr(ox)_3]ClO_4$ serve as model compounds for the unambiguous identification of the different mechanisms of energy migration within the ^2E state of the $[Cr(ox)_3]^{3-}$ chromophore [15].

2. The $^4A_2 \rightarrow {}^2E$ transition of Cr^{3+} in pseudo-octahedral coordination

The Cr^{3+} ($3d^3$) ion in octahedral or close to octahedral coordination, particularly in doped materials such as ruby, has been extensively studied by spectroscopists for over a hundred years and has played an important role in the development of ligand-field theory [16]. Thus, for weak ligand fields, the lowest excited state is a $^4T_2(t_{2g}{}^2e_g{}^1)$ state having the same spin multiplicity as the $^4A_2(t_{2g}{}^3)$ ground state, and for moderate to strong ligand fields the lowest excited state is the $^2E(t_{2g}{}^3)$ state having a different spin multiplicity but the same orbital occupancy as the ground state. In addition there are higher lying doublet and quartet ligand-field states. As a result the Cr^{3+} ion has comparatively strong visible absorption bands corresponding to spin-allowed ligand-field transitions from the $^4A_2(t_{2g}{}^3)$ ground state to the $^4T_2(t_{2g}{}^2e_g{}^1)$, $^4T_1(t_{2g}{}^2e_g{}^1)$ and $^4T_1(t_{2g}{}^1e_g{}^2)$ excited states and additional weak but sharp features at the edge to the near infrared corresponding to the multiplet of the $^4A_2(t_{2g}{}^3) \rightarrow {}^2E(t_{2g}{}^3)$ transition as well as to other doublet states at higher energies. For the $^4A_2 \rightarrow {}^4T_2$ transition, one electron is promoted to the anti-bonding e_g orbitals resulting in a marked elongation of the metal–ligand bond-length. On the other hand, the $^4A_2 \rightarrow {}^2E$ transition is a spin–flip transition, and consequently there are no important geometrical changes in the ^2E state with respect to the ground state, as is schematically shown in the configurational coordinate diagram in Fig. 1.

Upon excitation, deactivation may occur via different channels depending upon the ligand-field strength as well as the excitation energy [17]. Excitation into the higher lying spin-allowed bands mainly results in rapid non-radiative deactivation to the $^4T_2$ state. In turn, the $^4T_2$ state can undergo a radiationless intersystem crossing process to the ^2E state if the latter is the lowest excited state, or it can undergo a radiative or non-radiative transition down to the ground state if it is the lowest excited state. Finally for complexes in solution it can be involved in excited state chemical reactions, such as, for instance, photo-induced ligand exchange [17]. If the ^2E state is the lowest excited state, $^2E \rightarrow {}^4A_2$ luminescence is generally observed, at least at low temperatures. For small $^4T_2$–^2E energy gaps, this luminescence may be quenched via thermal population of the $^4T_2$ state [17,18].

In this study, emphasis will be on the $^4A_2 \rightarrow {}^2E$ transition and in particular on different mechanisms of non-radiative energy transfer processes that take place within this transition for chromium(III)

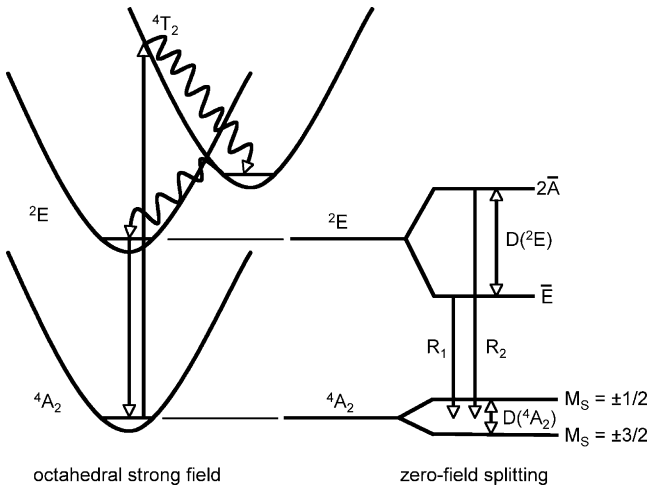

Fig. 1. Scheme of the ground state and the lowest excited ligand-field states of Cr^{3+} in a moderate to strong octahedral ligand field (left) and the zero-field splittings resulting from a trigonal distortion and spin–orbit coupling (right).

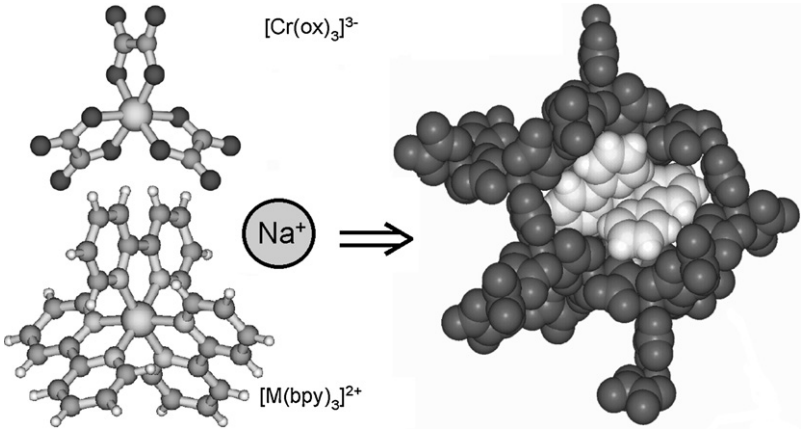

Fig. 2. The complexes $[Cr(ox)_3]^{3-}$ and $[M(bpy)_3]^{2+}$, and the three-dimensional oxalate network (black) encapsulating the tri-bipyridine cation (white) in $[M(bpy)_3][NaCr(ox)_3]$ (adapted from ref. [15a]).

in an oxygen environment. The excited-state dynamics of such systems have been studied in detail by Forster [18]. In ruby each Cr^{3+} is surrounded by a trigonally distorted (C_3) octahedron of six nearest neighbour oxygen atoms. All sites are crystallographically equivalent, $^4T_2$ is above ^2E and the gap $^4T_2$–^2E is quite large. As a result the $^2E \rightarrow {}^4A_2$ phosphorescence dominates up to 400 K. In emerald ($Be_3Al_2(SiO_3)_6$:Cr^{3+}) the $^4T_2$–^2E gap is smaller and consequently the phosphorescence is only observed up to 77 K. Above that temperature the broad fluorescence from the $^4T_2 \rightarrow {}^4A_2$ grows in intensity and dominates at 300 K.

In lower than octahedral symmetry, as, for instance, in the C_3 site symmetry of Cr^{3+} in ruby, both the $^4A_2$ ground state as well as the ^2E excited state are split by the combined effects of the lower symmetry and spin–orbit coupling, as schematically shown in Fig. 1. In ruby the zero-splitting splitting (ZFS) of the ^2E state is 29 cm^{-1} and easily resolved optically in both absorption and emission spectra, giving rise to the two R-lines. The ground state ZFS of 0.39 cm^{-1} is not so easily resolved in simple luminescence spectra. It can be determined by EPR spectroscopy [19] or by more sophisticated techniques such as fluorescence line narrowing spectroscopy [20–22] or spectral hole burning [21–23].

2.1. The model systems *[Ru(bpy)3][NaCr(ox)3]* and *[Rh(bpy)3][NaCr(ox)3]ClO4*

The $[Cr(ox)_3]^{3-}$ complex may be considered as chemist's version of ruby, with six-fold oxygen coordination and the tris-chelate complex having D_3 point group symmetry. As shown below, its spectroscopic properties are very similar to those of Cr^{3+} in ruby. However, as molecular unit, it can be incorporated into stoechiometric compounds, for instance, in the three-dimensional networks as model systems for studying different mechanisms of energy migration.

2.1.1. The crystal structure

The three-dimensional networks of the compounds $[Ru(bpy)_3][NaCr(ox)_3]$ and $[Rh(bpy)_3][NaCr(ox)_3]ClO_4$ crystallise in the cubic and chiral space group $P2_13$ with $Z = 4$ [24]. The site symmetry of all metal centres is C_3, that is, in the crystal structure the three-fold molecular axis of the tris-chelate complex is retained. As shown in Fig. 2, the three-dimensional network is formed by the $[Cr(ox)_3]^{3-}$ complexes bridged by the Na^+ ions, and it provides perfect cavities for the size and the geometry of the $[M^{II/III}(bpy)_3]^{2+}$ complexes. The structure of the oxalate network is effectively stabilised by the templating effect of the tris-bipyridine complexes through electrostatic interactions as well as $\pi\pi$ interactions between the oxalate and the bipyridine ligands. The chromium and the sodium ions are perfectly organised in an alternating fashion throughout the oxalate network. Thus, the chromium ions are never connected to each other directly by an oxalate bridge, and therefore super-exchange interactions between them are virtually non-existent [25]. This will have important consequences for energy migration.

2.1.2. Absorption and emission spectra

Fig. 3 shows the single crystal absorption spectrum of $[Zn(bpy)_3][NaCr(ox)_3]$ in the region of the ligand-field bands. It is essentially identical to the spectrum of $[Cr(ox)_3]^{3-}$ reported by Schmidtke and co-workers [26a] and Mortensen [26b]. The broad bands centred at 18,000 cm^{-1} and at 25,400 cm^{-1} are readily attributed to the spin-allowed $^4A_2 \rightarrow {}^4T_2$ and $^4A_2 \rightarrow {}^4T_1$ transitions, respectively. The weak and sharp features at 14,400, 14,800 and 21,000 cm^{-1} are attributed to the spin–flip transitions $^4A_2 \rightarrow {}^2E$, $^4A_2 \rightarrow {}^2T_1$ and $^4A_2 \rightarrow {}^2T_2$, respectively, which have their intensity concentrated in the electronic origins.

Fig. 4 shows the enlarged region of the electronic origins of the $^4A_2 \rightarrow {}^2E$ transition, that is, the R_1 and the R_2 lines, in absorption at 10.4 K for $[Rh(bpy)_3][NaCr(ox)_3]ClO_4$ and $[Ru(bpy)_3][NaCr(ox)_3]$, respectively. For the former, the ZFS of the ^2E state is 13.1 cm^{-1}, for the latter it is 13.7 cm^{-1}. The key difference between the spectra of

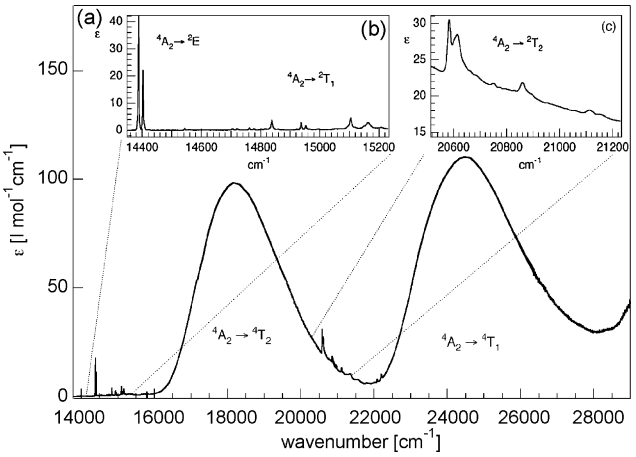

Fig. 3. Single crystal absorption spectrum of $[Zn(bpy)_3][NaCr(ox)_3]$ at 10.4 K: (a) full spectrum, (b) the $^4A_2 \rightarrow {}^2E$ and $^4A_2 \rightarrow {}^2T_1$ transitions and (c) the $^4A_2 \rightarrow {}^2T_2$ transition.

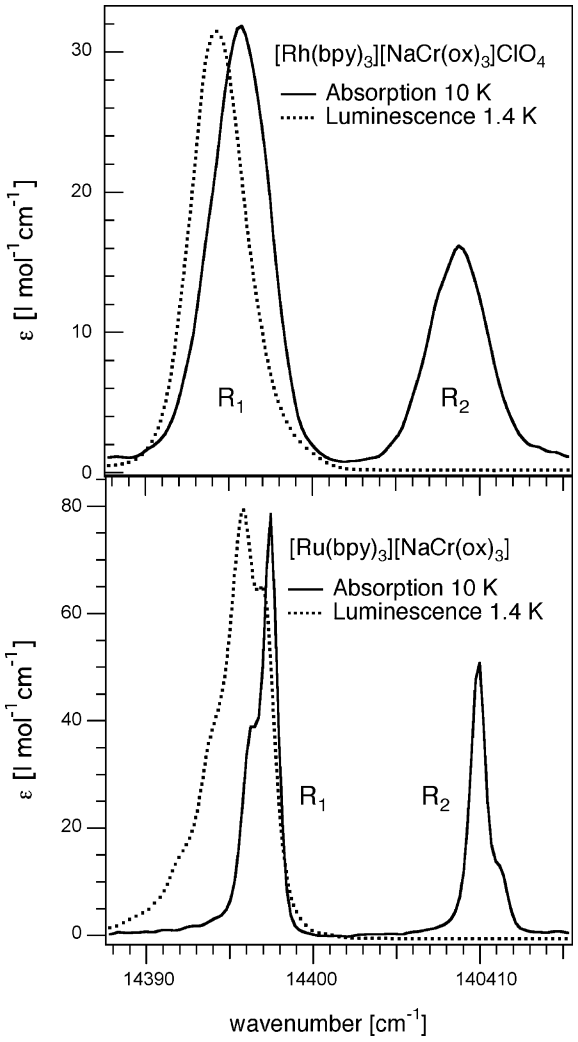

Fig. 4. The $^4A_2 \rightarrow {}^2E$ transition in absorption at 10.4 K (—) and in emission at 1.4 K (. . .) for $[Rh(bpy)_3][NaCr(ox)_3]ClO_4$ (top) and $[Ru(bpy)_3][NaCr(ox)_3]$ (bottom) single crystals. For the latter, the fit of two Gaussians to the R lines in absorption is included.

the two compounds lies in the inhomogeneous line width resulting from non-equivalent static distortions in the crystalline environment of the chromophores. Whereas for $[Rh(bpy)_3][NaCr(ox)_3]ClO_4$ it is approximately 4.3 cm^{-1}, it is considerably smaller for $[Ru(bpy)_3][NaCr(ox)_3]$. The oscillator strengths, however, are identical, and for R_1 a value of 6×10^{-7} can be derived from standard theory [27]. The shoulders in both R lines of the ruthenium(II) compound indicate that for this compound the ZFS of the $^4A_2$ ground state is on the verge of being resolved. A least squares fit with a sum of two Gaussians to both R lines give a value of 1.29(7) cm^{-1} for the ground state ZFS and a inhomogeneous line width of 1.1(1) cm^{-1}. This value of the ZFS is in line with values determined by EPR spectroscopy [28] and high-resolution optical methods [29], which also identified the $M_S = \pm 3/2$ component of the $^4A_2$ multiplet as the ground state.

Fig. 4 includes the luminescence observed at 1.4 K upon non-selective excitation into the $^4T_2$ absorption band of the $[Cr(ox)_3]^{3-}$ chromophore at 18,416 cm^{-1} (543 nm). The narrow band luminescence is assigned to the $^2E \rightarrow {}^4A_2$ transition and is fed via efficient intersystem crossing from the $^4T_2$ state. At 1.4 K only the lower component of the ^2E state is populated and therefore only the R_1 line is observed. For both compounds and in contrast to diluted systems, the luminescence is slightly shifted to lower energies with respect to the absorption. This gives a first indication that in these highly concentrated systems energy migration is indeed important. In addition, the emission from $[Ru(bpy)_3][NaCr(ox)_3]$ shows a weak structure with multiple spacings corresponding to the ZFS of the ground state.

In contrast to ruby for which the luminescence quantum efficiency is close to unity from cryogenic temperatures all the way up to room temperature, this is not the case for the oxalate networks. Even when doped into inert host lattices such as $[Rh(bpy)_3][NaAl(ox)_3]ClO_4$ where Cr^{3+} substitutes for Al^{3+}, the luminescence is quenched at $T > 100$ K. This is due to rapid non-radiative multiphonon relaxation via thermally activated back-intersystem crossing to the $^4T_2$ state [30]. Nevertheless, at $T < 50$ K, the luminescence quantum efficiency in such dilute systems approaches unity as borne out by the observed luminescence lifetime in diluted systems of 1.3 ms [15], that is, close to the radiative lifetime estimated from the oscillator strength, again according to standard theory [27]. In the concentrated oxalate networks, the luminescence intensity decreases rapidly above 4.2 K, another indication for rapid energy migration and quenching by killer traps present at low concentrations even if ultra pure chemicals are used in the synthesis.

2.2. Electronic origins, homogeneous line widths and inhomogeneous broadening

The ultimate line width called the homogenous line width Γ_{hom} of an electronic origin having a Lorentzian lineshape is given by its total dephasing time T_2 according to

$$\Gamma_{hom} = \frac{1}{\pi T_2} = \frac{1}{\pi}\left(\frac{1}{2T_1} + \frac{1}{T_2^*}\right) \quad (1)$$

where T_2^* is the pure dephasing time and T_1 is the lifetime of the excited state level. T_1 contains all processes affecting the lifetimes of the levels in question and should not be confused with the observed luminescence lifetime. For a comprehensive discussion of the different contributions to T_2^* with special emphasis on transition metal complexes, the reader is referred to the excellent reviews by Riesen [31], who states that at low temperatures in diamagnetic systems, T_2^* is usually quite large and can thus be neglected as contribution to Γ_{hom}, but in paramagnetic systems electron-spin–electron-spin and electron-spin–nuclear spin interactions substantially shorten T_2^* and thus contribute to the residual homogeneous line width at low temperatures. At temperatures above ~6 K, dephasing due to electron–phonon interactions become the dominant contribution to Γ_{hom} [6].

For most Cr^{3+} chromophores it is difficult to accurately determine the ZFS by conventional optical spectroscopy because at low temperatures the inhomogeneous distribution even in high quality crystals is often not only much larger than the homogeneous line width, it is also larger than the ZFS. As mentioned above, an alternative to EPR spectroscopy is provided by fluorescence line narrowing (FLN) spectroscopy [18–22,31]. The principle is shown schematically in Fig. 5. A narrow band laser, tuned to the electronic origin of interest, selectively excites only a subset of chromophores within the inhomogeneously broadened band. For the $^4A_2 \rightarrow {}^2E$ transition in the absence of energy transfer processes, a typical three-line spectrum is observed as, for instance, in the FLN spectrum of $[Cr(ox)_3]^{3-}$ doped into $[Rh(bpy)_3][NaAl(ox)_3]ClO_4$ included in Fig. 5. The central line is the resonant line and corresponds to the emission of the selectively excited chromophores back to the ground state component from which they were excited. The two satellites are non-resonant lines and are shifted to lower and higher energy by the ground state ZFS, the latter being a hot band result-

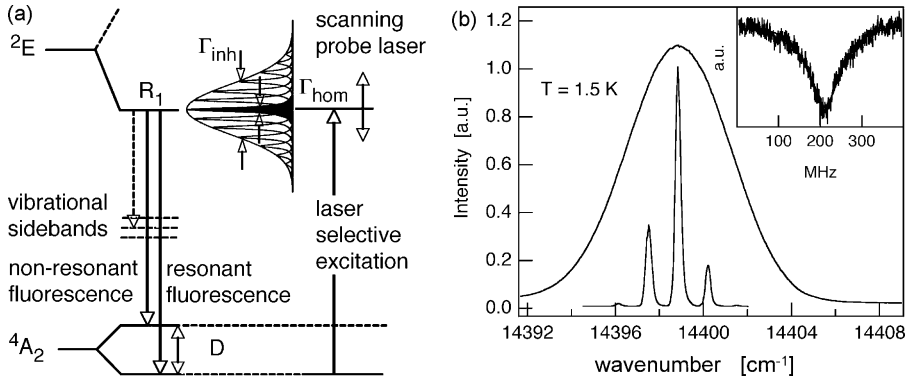

Fig. 5. (a) The principle of fluorescence line narrowing using laser selective excitation exciting a subset of complexes within the inhomogeneously broadened electronic origin. In order to prevent laser light from the excitation source from entering the detection system, the excitation source is chopped at a comparatively high frequency and the luminescence light is only collected during the dark time of the excitation source. For transient spectral hole burning, a single frequency pump laser is kept at a fixed frequency keeping up a steady state population in the excited state. This spectral hole is probed by a second single frequency laser, which is scanned across the corresponding spectral range. Detection can be either done by direct transmission or in an excitation type configuration using the vibrational side bands of the emission. (b) Non-selective luminescence and FLN spectrum at 1.5 K of $[Rh(bpy)_3][NaAl(ox)_3]ClO_4$ doped with 0.5% Cr^{3+}. (Inset) Transient spectral hole of the resonant line.

ing from the excitation from the Ms = ±1/2 component of the $^4A_2$ state. Indeed, the FLN spectrum confirms the ZFS of 1.3 cm^{-1} as determined above for $[Ru(bpy)_3][NaCr(ox)_3]$ by conventional spectroscopy.

In the above FLN spectra, the spectral resolution is limited to 0.25 cm^{-1} (8 GHz) by the 3/4 m double monochromator used for light-dispersion. This is several orders of magnitude larger than the homogeneous line width. A versatile technique for determining homogeneous line widths is spectral hole burning [21–23,31]. In spectral hole burning a subset of chromophore is depleted in the ground state upon selective laser excitation, resulting in a persistent or transient dip in the absorption or excitation spectrum. A transient ground state depletion can be monitored with a second laser, which is scanned at lower power across the wavelength of the pump beam. The inset of Fig. 5 shows such a spectral hole recorded in excitation mode under continuous irradiation by the pump beam into the R_1 line of $[Rh(bpy)_3][NaAl(ox)_3]ClO_4$ doped with 0.5% Cr^{3+} at 1.5 K. The line shape is close to Lorentzian with an observed line width Γ_{obs} of 40 MHz. Spectral hole burning is a sequential two photon process: the first photon is used to burn the hole, the second photon is used in the readout process. Therefore, the homogenous line width Γ_{hom} corresponds to $\Gamma_{obs}/2$. Thus, in the lightly doped oxalate network at low concentration the homogeneous line width is 20 MHz at 1.5 K. This is in line with the value determined for the $NaMg[Al(ox)_3]\cdot 9H_2O$ host lattice doped with 1% Cr^{3+} by Lewis and Riesen [29], who also used hole burning spectroscopy in weak magnetic fields to unambiguously show that the Ms = ±3/2 component of the $^4A_2$ state is the true ground state of $[Cr(ox)_3]^{3-}$ and to determine ground and excited state g-values to high precision [32]. Riesen and co-workers also showed that the residual homogeneous line width of the R_1 becomes orders of magnitude smaller in a magnetic field due to the reduction in electron-spin–electron-spin relaxation, which is the main dephasing mechanism at low temperatures even in comparatively lightly doped materials [32], since spin–lattice relaxation times within the components of the $^4A_2$ ground state are of the order of milliseconds at low temperatures [33].

Accordingly, in more concentrated systems, homogeneous line widths are larger than in diluted system due to spin–spin relaxation. As shown in Fig. 6 for T = 1.5 K, Γ_{hom} increases in a sigmoidal fashion from the initial 20 MHz (~0.0007 cm^{-1}) at x = 0.5% to a limiting value of ~600 MHz (~0.02 cm^{-1}) at x = 100%. The latter value may be considered as upper limit as it probably overestimates the true value since at high concentrations resonant energy migration (see below) within one subset may result in additional broadening of the observed line width in the hole burning experiment.

As likewise shown in Fig. 6, the homogeneous line width is temperature dependent, increasing rapidly above 4.2 K, in particular

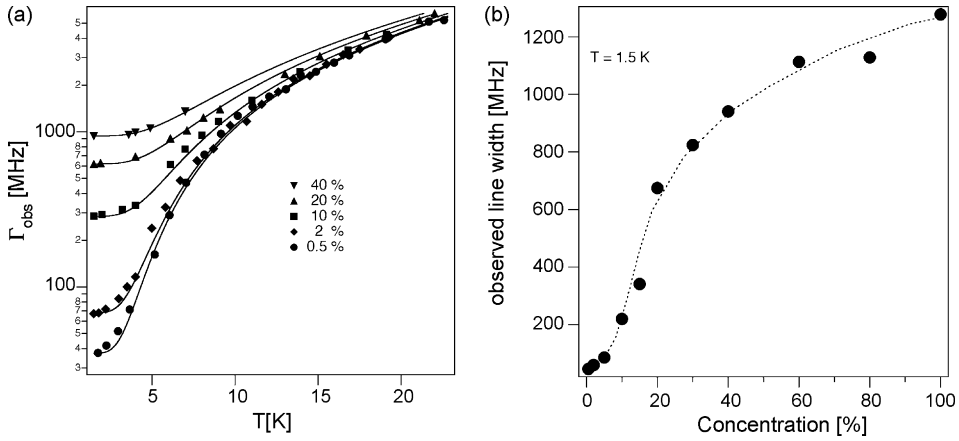

Fig. 6. (a) The observed line width $\Gamma_{obs} = 2\Gamma_{hom}$ in transient hole-burning under steady state excitation as a function of temperature for the mixed crystals $[Rh(bpy)_3][NaAl_{1-x}Cr_x(ox)_3]ClO_4$ (x = 0.005, 0.2, 0.1, 0.2 and 0.4). (b) The observed line width Γ_{obs} as a function of the mole fraction x at 1.5 K.

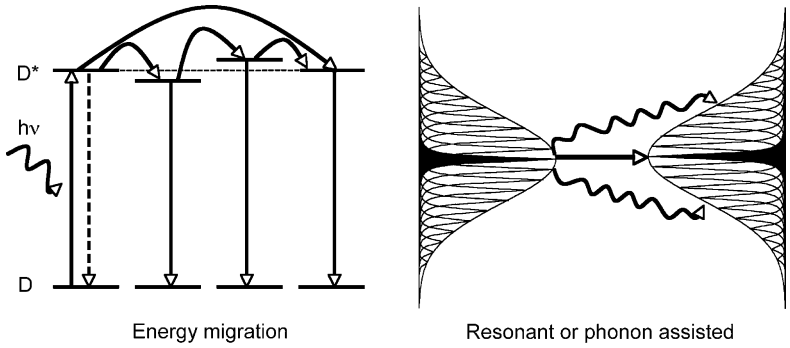

Fig. 7. Schematic representation of excitation energy migration at high chromophore concentration: as a result of the inhomogeneous distribution, the transfer to nearest neighbours is not resonant and requires the creation or annihilation of phonons to bridge the energy mismatch. Resonant transfer is only possible between truly resonant chromophores within the inhomogeneous distribution and these are not usually nearest neighbours.

for the diluted system. This is due to phonon-assisted relaxation processes such as direct absorption or emission of phonons, and Raman and Orbach processes [6] basically within the two components of ^{2}E state. As shown by Riesen, for $[Cr(ox)_3]^{3-}$ [29] and similar chromium(III) complexes [34], both the direct process as well as Raman processes contribute to the homogeneous line width above 4.2 K. In contrast, for ruby Raman processes dominate at higher temperatures [35,22]. The key difference between the otherwise very similar chromphores lies in the density of phonon states at the energies of the ^{2}E ZFS, which is much higher for the softer oxalate systems with a Debye temperature of around 50 K [36] as compared to 950 K for ruby [37]. The fact that in the dilute oxalate network the homogeneous line width increases more rapidly than in the $NaMgAl(ox)_3{\cdot}9H_2O$ host investigated by Lewis and Riesen [29] is due to the smaller ZFS of 13.2 cm^{-1} as compared to 20 cm^{-1} for the latter. For a comprehensive discussion of the homogeneous line width as a function of temperature the reader is referred to ref. [31]. For the present discussion it is important to note that for the concentrated oxalate network the homogeneous line width is dominated by spin–spin relaxation up to ~5 K and is thus almost constant below that temperature.

3. Theoretical aspects of energy migration

As discussed above, at low temperatures the homogeneous line width of electronic origins is usually several orders of magnitude smaller than the inhomogeneous distribution even in high-quality crystalline materials and at high chromophore concentrations. Thus, the question to be asked is, is the energy migration a truly resonant process, with the initially excited chromophore looking for a partner with which it is electronically resonant within one homogeneous line width, or is the energy transferred to the nearest neighbour, with which it is not necessarily resonant, and the energy mismatch is made up by the creation or annihilation of phonons as schematically shown in Fig. 7. Even though energy migration in crystalline materials with high dopant concentrations was found to be dominated by phonon-assisted processes in a majority of cases, the following discussion begins with the resonant process, this in view of the extraordinary behaviour of the model systems to be discussed in Section 4.

3.1. Resonant energy transfer

The dominant contribution to the electronic interaction for resonant energy transfer is most often the electric-dipole–electric-dipole interaction between the respective transition dipole moments. The corresponding rate constant can be cast in the well-known form (in SI units) [6]

$$w_{DA} = \left(\frac{1}{4\pi\varepsilon_0}\right)^2 \left(\frac{3\hbar e^4}{4\pi n^4 m^2}\right) \times \frac{\kappa^2 f_D f_A \Omega_{DA}}{R_{DA}^6 \nu_{DA}^2} = \frac{1}{\tau_D}\left(\frac{R_c}{R_{DA}}\right)^6 \quad (2)$$

where τ_D is the intrinsic luminescence lifetime of the donor in the absence of any acceptor chromophores, R_{DA} is the donor–acceptor separation, and R_c is the critical radius given by

$$R_c = \left(\text{Const} \times \frac{\kappa^2 f_A \Omega_{DA} \eta_D^r}{\tilde{\nu}_{DA}^4}\right)^{1/6} \quad (3)$$

In Eq. (3), f_A is the dimensionless oscillator strength of the acceptor transition, η_D^r is the luminescence quantum efficiency of the donor transition, $\tilde{\nu}_{DA}$ is the mean energy at which the transfer takes place, and κ^2 is a geometrical factor, which averaged over all possible orientations takes on a value of 2/3. Ω_{DA} is the spectral overlap integral of the normalised line shape functions of the donor emission, g_D, and the acceptor absorption, g_A, and is given by

$$\Omega_{DA} = \int g_A(\tilde{\nu}) g_D(\tilde{\nu})\, d\tilde{\nu} \quad (4)$$

It takes care of energy conservation. Const regroups all the fundamental quantities, including the ones appearing upon substitution of the oscillator strength of the donor transition by the proportionality $f_D \sim 1/\tau_D^r = \eta_D^r/\tau_D$ [27]. For $\tilde{\nu}_{DA}$ in wave numbers, a typical value for the index of refraction $n = 1.7$ for the compounds in question, and R_c in Å, Const $\approx 10^{31}$. The physical significance of the critical radius is that at an effective donor–acceptor separation $R_{DA} = R_c$, the probability for excitation energy transfer is equal to the probability of luminescence of the donor, that is, the quantum efficiency for energy transfer $\eta_{DA}^{et} = 0.5$.

With respect to energy migration, the spectral overlap is restricted to the electronic origin of the corresponding transition. Thus, efficient resonant energy migration is only to be expected for systems with small Stokes' shifts and Huang–Rhys factors close to zero. The $^4A_2 \rightarrow {}^2E$ spin–flip transition of Cr^{3+} should thus be ideally suited for energy migration studies. However, at low temperatures the homogeneous line width of the electronic origins is much smaller than the inhomogeneous distribution. Thus, only those chromophores within a homogenous line width of each other inside the inhomogeneous distribution can transfer the energy resonantly. For such truly resonant chromophores, the maximum spectral overlap integral can be expressed as

$$\Omega_{DA} = \int [g(\tilde{\nu})]^2\, d\tilde{\nu} = \frac{1}{\pi \Gamma_{hom}} \quad (5)$$

where $g(\nu)$ is the Lorentzian lineshape function with the corresponding homogeneous line width Γ_{hom}. Using the value for the

homogeneous line width of concentrated materials of the order of $\Gamma_{hom} \leq 0.02\,cm^{-1}$ (600 MHz) at 1.5 K, and an oscillator strength of the spin and parity forbidden $^4A_2 \rightarrow {}^2E$ transition of $\sim 6 \times 10^{-7}$, Ω_{DA} and R_c take on values of 16 cm and 34 Å, respectively. It is interesting to note that the value for R_c is of the order of the values found for the best donor–acceptor pairs used in FRET studies with organic dyes [38] despite the fact that the $^4A_2 \rightarrow {}^2E$ transition is both parity as well as spin-forbidden. This is due to the much larger value of the spectral overlap integral as compared to the one found for the large absorption and emission bands of the organic dyes, which counteracts the small value of the oscillator strength of the acceptor.

In order for energy migration to proceed via such a resonant process the concentration of chromophores, which are resonant within one homogenous line width inside the inhomogeneous distribution must be sufficiently large. At the centre of the inhomogeneous distribution, this concentration is simply given by the ratio of the homogenous to the inhomogeneous line width according to

$$N_{res} = \frac{2\Gamma_{hom}}{\Gamma_{inh}} N_{tot} \quad (6)$$

where N_{tot} is the total concentration of chromophores and the factor of 2 takes into account the partial spectral overlap between spectral neighbours within the inhomogeneous distribution. With this the mean number of resonant or quasi-resonant chromophores, n_m, within a sphere of radius R_c can be estimated as a function of both Γ_{hom} and Γ_{inh}

$$n_m = \frac{2\Gamma_{hom}}{\Gamma_{inh}} N_{tot} \frac{4\pi}{3} R_c^3 \quad (7)$$

in which R_c is a function of Γ_{hom} according to Eqs. (3) and (5), and thus $n_m \sim \sqrt{\Gamma_{hom}}/\Gamma_{inh}$. Fig. 8 shows the mean number of resonant chromophores at the centre of the inhomogeneous distribution as function of the homogeneous line width with the inhomogeneous line width as parameter and taking $N_{tot} = 10^{21}\,cm^{-3}$, which corresponds to the concentration of the neat model compounds or a 1% Cr^{3+} doped ruby. For a homogeneous line width of $0.02\,cm^{-1}$, the critical inhomogeneous width is around $4\,cm^{-1}$. For larger inhomogeneous distributions, the concentration of resonant species becomes too small, and the resonant process cannot be efficient, for narrower distributions, it can, in principle, become very efficient

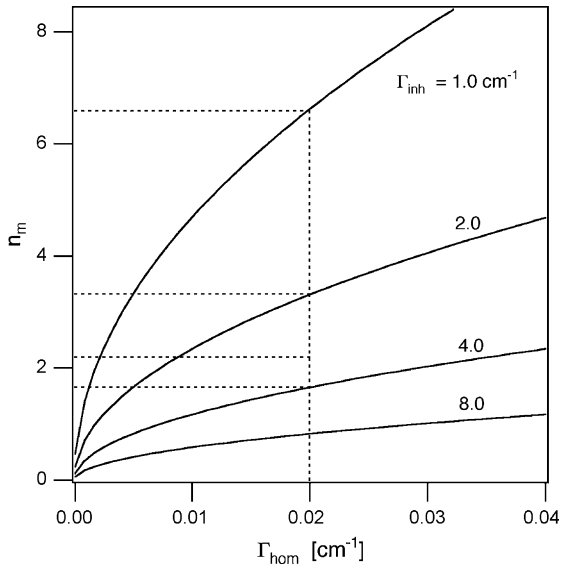

Fig. 8. Mean number of resonant chromophores at the centre of the inhomogeneous distribution as a function of the homogeneous line width Γ_{hom} for different values of the inhomogeneous line width Γ_{inh}.

as on average there are more than two resonant species within a sphere of R_c. As will become evident in the discussion on energy migration in the model compounds, namely the three-dimensional oxalate networks, the above is of utmost importance. In contrast, in the much-studied doped oxides, resonant processes are of lesser importance.

3.2. Phonon-assisted energy transfer

As mentioned above, at low temperature two spatially nearest neighbour chromophores are not necessarily spectral neighbours within the inhomogeneously broadened band. As a result, the spectral overlap integral is usually very small and resonant energy migration between nearest neighbours does not occur. However, the small energy mismatch can be made up by the creation and annihilation of phonons in phonon-assisted processes. Similar to the processes responsible for the increase in homogeneous line width at higher temperatures, these can occur in a direct process with the annihilation or creation of a single phonon, or in Orbach and Raman processes which are two-phonon processes. In view of the small energy mismatch of $\sim\Gamma_{inh}$ to be bridged by the phonon-assisted process, the latter two are more likely [12]. Irrespective of the mechanism, phonon-assisted energy migration is strongly temperature dependent and usually freezes below ~10 K.

4. Energy migration within the $^4A_2 \rightarrow {}^2E$ transition

4.1. Al_2O_3:Cr^{3+} and other doped systems

The $^4A_2 \rightarrow {}^2E$ transition Cr^{3+} in ruby is probably the most studied transition of any transition metal ion of the periodic table, and a large number of fundamental phenomena were discovered using ruby. Among these, excitation energy transfer and migration and the discussion of the possible mechanisms play a key role [14]. The luminescence spectrum of ruby is dominated by the two R-lines corresponding to emission from isolated Cr^{3+} centres, but already at comparatively low Cr^{3+} concentrations additional lines, the so-called N-lines appear at lower energies. These have been attributed to exchange coupled pairs of Cr^{3+} ions [39] with different bridging geometries. Thus, a number of different energy transfer processes have to be considered: the energy migration within the ^2E state of the isolated Cr^{3+} centres, and the transfer from isolated centres to the different exchange coupled pairs as final acceptors [14,40]. As the relative concentration of exchange coupled pairs and the homogeneous as well as the inhomogeneous line widths of the single ions all vary with the Cr^{3+} concentration, and as the inhomogeneous line width furthermore depends upon the crystal quality and the homogeneous line width upon temperature, the problem of energy migration in ruby becomes a multi-parameter problem. Indeed, the discussion on the mechanisms of the various energy transfer processes has been controversial. Time-resolved FLN experiments show that above ~10 K, energy migration is dominated by phonon-assisted processes [41]. However, the nature of the processes could not be answered unambiguously. More importantly, the initially postulated fast resonant energy migration between resonant single ions at low temperatures [40,42] was later shown to be incorrect by Jessop and Szabo [43] and Chu et al. [44], who showed it to occur on a millisecond timescale. Indeed, according to the above arguments, a Cr^{3+} concentration of >1 mol% would be required to achieve a sufficient concentration of resonant species. However, at such concentrations, the concentration of exchange coupled pairs becomes so high that the energy is quickly transferred to these, where it remains trapped.

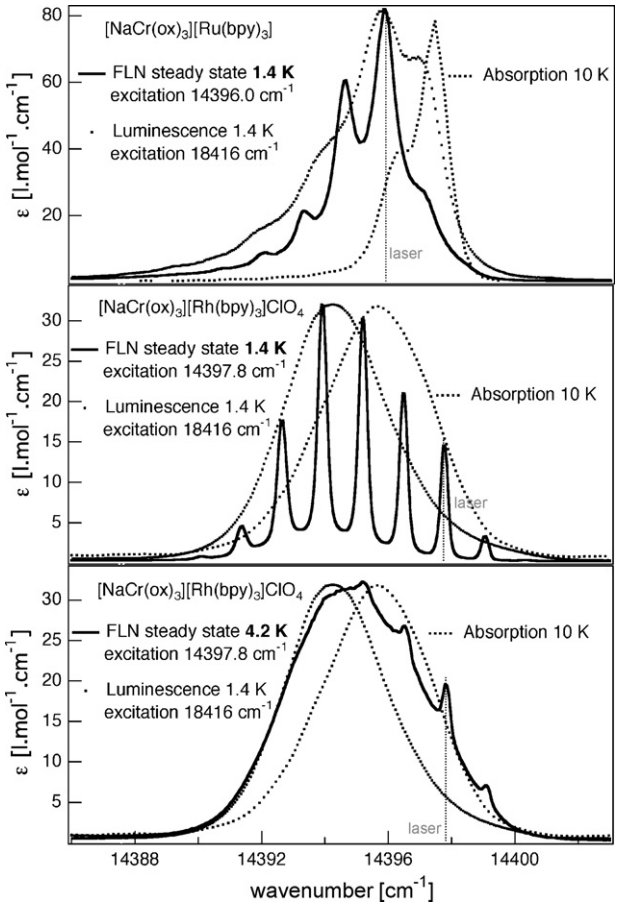

Fig. 9. Steady state FLN spectra of the R_1 line of the $^4A_2 \rightarrow {}^2E$ transition of (top) $[Ru(bpy)_3][NaCr(ox)_3]$ at 1.4 K, (middle) of $[Rh(bpy)_3][NaCr(ox)_3]ClO_4$ at 1.4 K and (bottom) at 4.2 K. The R_1 absorption and the non-selective emission spectra are included for direct comparison.

As another example of a doped oxide, emerald ($Be_3Al_2(SiO_3)_6:Cr^{3+}$) has been studied by Hasan et al. [45]. Emerald has the beryl structure, the site symmetry of Cr^{3+} is D_3. In emerald, the nearest-neighbour Al^{3+} sites are 4.6 Å apart whereas in ruby the distance is only 2.65 Å. Exchange interactions are thus negligible. In contrast to ruby, the energy transfer in emerald has been clearly established to be two-phonon-assisted and dipole–dipole in nature, in line with a number of other materials [46] as well as with theoretical considerations [12].

4.2. With $[Cr(ox)_3]^{3-}$ as chromophore in three-dimensional oxalate networks

The steady state FLN spectra at 1.4 K for excitation into the R_1 line of the $^4A_2 \rightarrow {}^2E$ transition of both $[Rh(bpy)_3][NaCr(ox)_3]ClO_4$ and $[Ru(bpy)_3][NaCr(ox)_3]$ are shown in Fig. 9 together with the non-selective R_1 emission and absorption. For the former, the excitation wavelength for FLN was tuned to slightly higher energy than the maximum of the absorption, for the latter to slightly lower energy. For $[Rh(bpy)_3][NaCr(ox)_3]ClO_4$, the FLN spectrum consists of more lines than the simple three-line spectrum spaced by the ground state ZFS. Indeed, up to eight narrowed lines with spacings between adjacent lines corresponding to $D = 1.3\ cm^{-1}$ are observed [15]. Thus, even though more than the expected three lines are observed, some energy selectivity is preserved in this compound at 1.4 K. For $[Ru(bpy)_3][NaCr(ox)_3]$ on the other hand, the selectivity seems to be lost to a large extent. The FLN spectrum is much more similar to the broadened emission spectrum with non-selective excitation. At elevated temperature any energy selectivity in the FLN spectrum is likewise lost even for $[Rh(bpy)_3][NaCr(ox)_3]ClO_4$, as demonstrated by the steady state FLN spectra recorded at 4.2 K included in Fig. 9. This behaviour is characteristic for energy non-selective phonon-assisted energy migration.

But how is the very different low-temperature behaviour of the two compounds to be explained? Further experimental evidence is provided by time-resolved FLN spectra following pulsed excitation shown in Figs. 10 and 11. For $[Rh(bpy)_3][NaCr(ox)_3]ClO_4$ the 1.4 K spectrum at the shortest delay of 30 μs is very close to the three-line spectrum for isolated chromophores. The additional lines appear sequentially at longer delays. As schematically shown in Fig. 12, this is explained by energy transfer in which the initially excited chromophore as donor gives the energy of its transition from the excited state to the upper component, that is, the $M_S = \pm 1/2$ component of the ground state, to an acceptor within the inhomogeneous distribution for which the transition from the $M_S = \pm 3/2$ component to the excited state is resonant. In turn the acceptor becomes the donor for the next step in handing the energy down the ladder spaced by the ZFS of the ground state. For $[Ru(bpy)_3][NaCr(ox)_3]$ the 1.4 K spectrum at the shortest delay of 30 μs is likewise very close to the three-line spectrum for isolated chromophores, and at longer delays some additional lines appear, however the total number is lower. This is to be expected, as the inhomogeneous line width of the ruthenium(II) containing compound is only $1.1\ cm^{-1}$ as compared to $4.4\ cm^{-1}$ for the rhodium(III) compound, and thus less multiples of the ground state ZFS can be accommodated within the inhomogeneously broadened band. The important difference is that in addition to the appearance of new lines, the initially sharp lines broaden out rapidly for longer delays. This is not due to phonon-assisted energy migration. The phonon-assisted process being totally frozen in at 1.4 K for the rhodium(III) compound, there is no reason as to why it should be so much faster in the ruthenium(II) compound. Indeed, the narrower inhomogeneous distribution would slow it down rather than accelerate it. Additionally, the evolution of the band shape is very much different from the one typical for the phonon-assisted process observed at higher temperature. As shown in Fig. 10, the non-energy selective phonon-assisted process in the rhodium(III) compound manifests itself as an increasingly rapid growing in of the full inhomogeneously broadened band without affecting the band width or the temporal evolution of the sharp bands, whereas in the ruthenium(II) compound at l.4 K the individual sharp line broadens out. This broadening has its origin in quasi-resonant energy migration between spectral neighbours due to partial overlap between the respective Lorentzians as schematically shown in Fig. 12. Curve fitting of the multi-line spectra with a set of Lorentzians spaced by $1.3\ cm^{-1}$ results in the evolution of the line width as function of delay time displayed in Fig. 13 for both compounds. Whereas the line width of the individual sharp lines for $[Rh(bpy)_3][NaCr(ox)_3]ClO_4$ stays almost constant at the value of the spectral resolution of the spectrometer of $0.2\ cm^{-1}$, for $[Ru(bpy)_3][NaCr(ox)_3]$ it increases rapidly from that value to reach almost the limiting value of $1.1\ cm^{-1}$ of the inhomogeneous line width for this compound. The question remains, why is the behaviour of the two compounds at 1.4 K so very different. As noted before, the key difference lies in their inhomogeneous line widths. With reference to Fig. 8, at a homogenous line width of $0.02\ cm^{-1}$, for $[Rh(bpy)_3][NaCr(ox)_3]ClO_4$ there are approximately 1.5 acceptors available for either the stepwise resonant or the quasi-resonant energy migration within the same component of the ground state. For $[Ru(bpy)_3][NaCr(ox)_3]$ there are more than 6, provided the homogeneous line widths in the two compounds are similar. In the present case and according to the Inokuti and

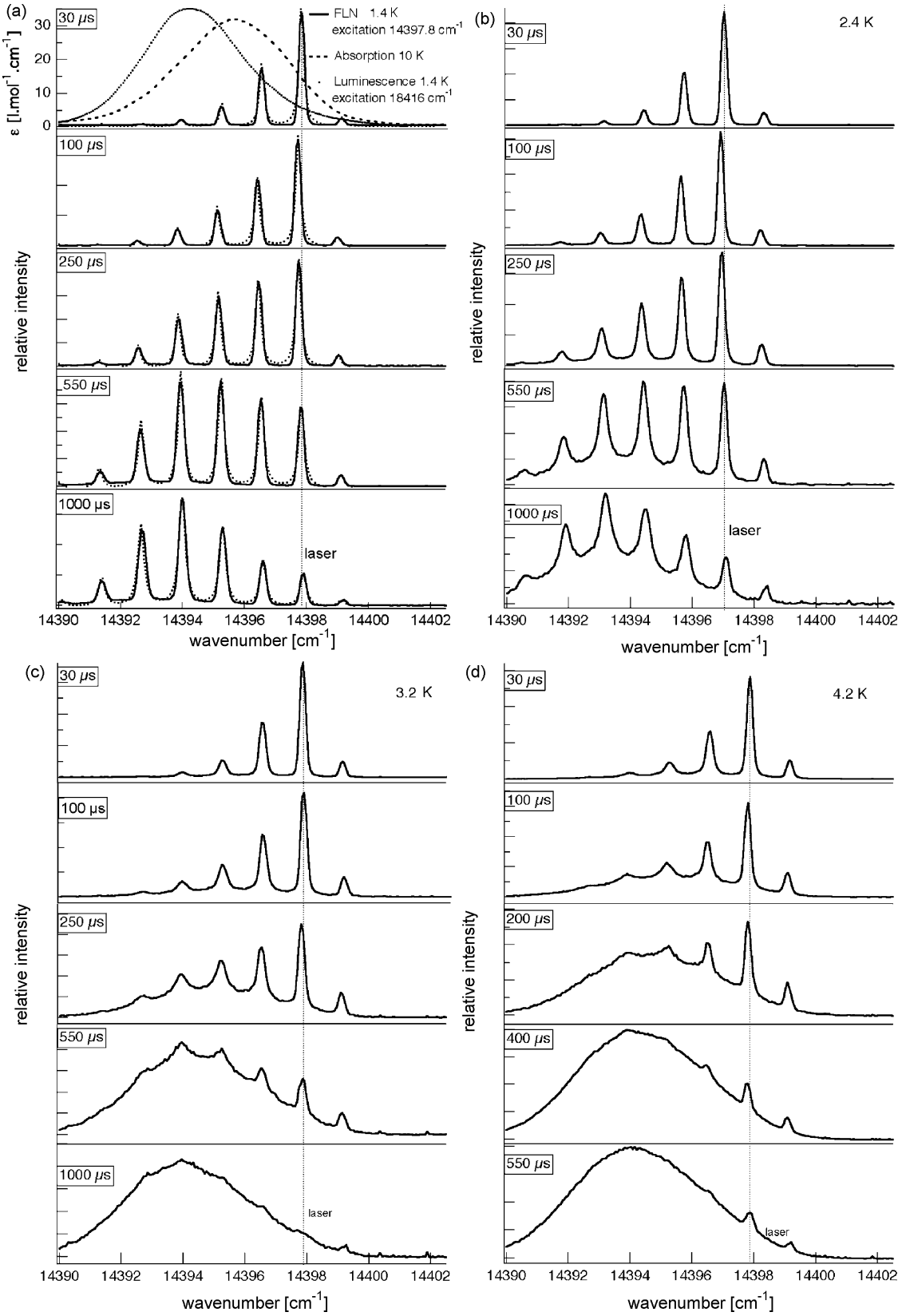

Fig. 10. Time-resolved FLN spectra of the R_1 line of the $^4A_2 \rightarrow {}^2E$ transition of $[Rh(bpy)_3][NaCr(ox)_3]ClO_4$ at different temperatures: (a) 1.4 K, (b) 2.4 K, (c) 3.2 K and (d) 4.2 K. The steady state FLN spectra as well as absorption and the non-selective emission spectra are included.

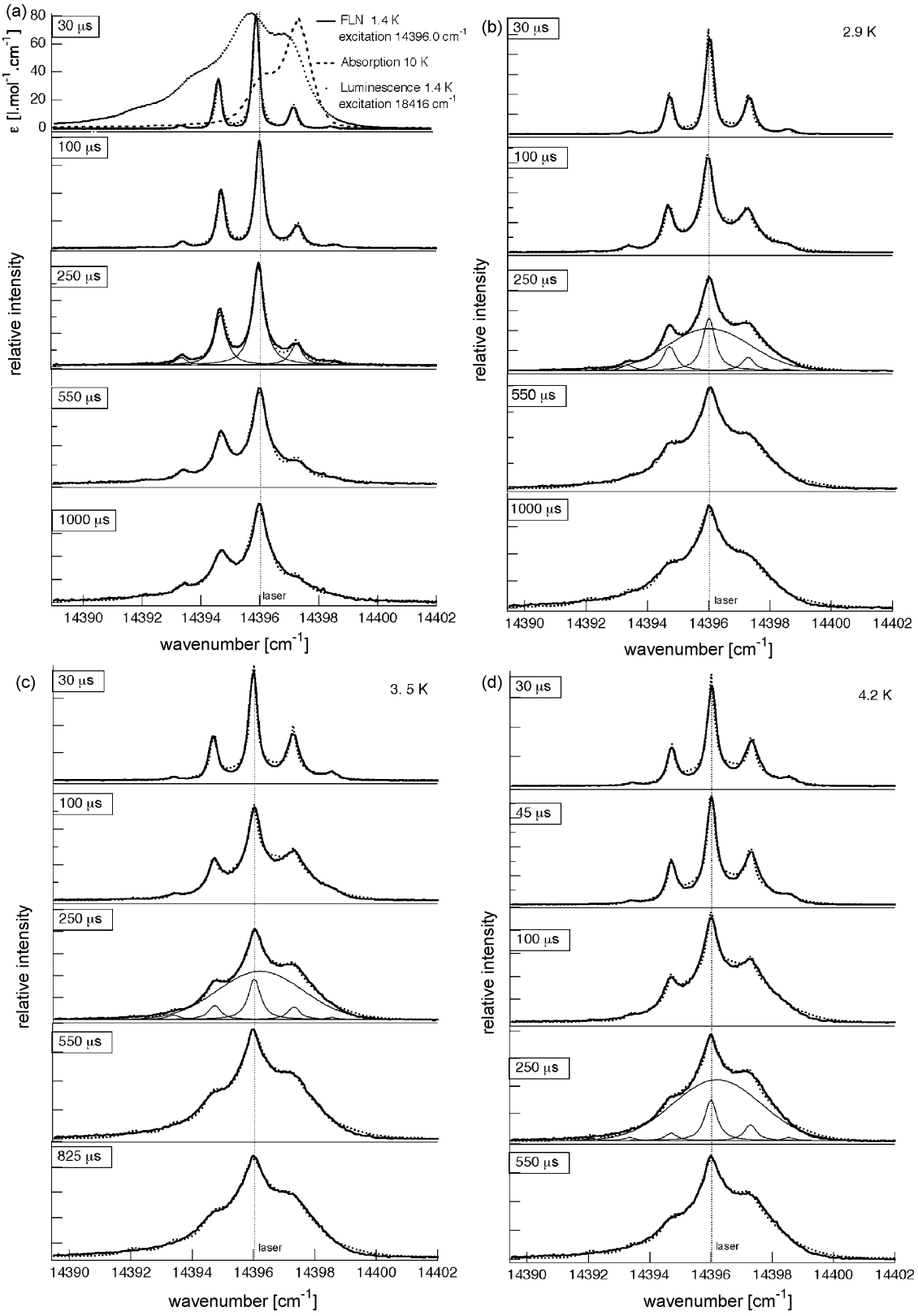

Fig. 11. Time resolved FLN spectra of the R_1 line of the $^4A_2 \rightarrow {}^2E$ transition of $[Ru(bpy)_3][NaCr(ox)_3]$ at different temperatures: (a) 1.4 K, (b) 2.9 K, (c) 3.5 K and (d) 4.2 K. The steady state FLN spectra as well as absorption and the non-selective emission spectra are included.

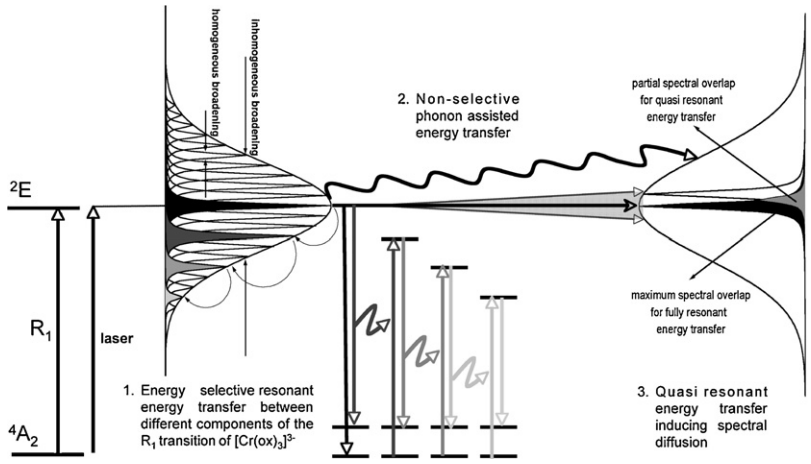

Fig. 12. Schematic presentation of the three mechanisms for energy migration in the three-dimensional oxalate networks. (1) Resonant energy transfer between different components of the ground state giving rise to a multi-line spectrum with spacings corresponding to the ground state ZFS. (2) Non-energy selective phonon-assisted energy migration between spatial neighbours at elevated temperature resulting in a growing inhomogeneous back-ground spectrum. (3) Quasi-resonant energy migration between spectral neighbours resulting in spectral diffusion around the resonant line.

Hirayama equation [47], an increase in the concentration of potential acceptors of a factor of four results in an increase of the energy transfer efficiency of at least an order of magnitude. Whereas for $[Rh(bpy)_3][NaCr(ox)_3]ClO_4$, a pseudo-first-order rate constant for the resonant energy transfer process of $k_{et}^{r} \approx 10^4\ s^{-1}$ had been estimated [15], this must therefore be of the order of $10^5\ s^{-1}$ for $[Ru(bpy)_3][NaCr(ox)_3]$. Or in other words, on average the energy is transferred ~100 times before radiative decay. With each step adding approximately $\Gamma_{hom} \approx 0.02\ cm^{-1}$ to the observed line width in the FLN spectrum, this explains the evolution of the observed line width from 0.2 cm^{-1} at 30 μs delay all the way to the full inhomogeneous width of 1.1 cm^{-1} at longer delays $[Ru(bpy)_3][NaCr(ox)_3]$, as well as the negligible increase for $[Rh(bpy)_3][NaCr(ox)_3]ClO_4$, for which the observed line width is limited by the spectral resolution of the monochromator.

Within the temperature interval of 1.4–4.2 K, the resonant processes are independent of temperature, as born out by the time-resolved FLN spectra at higher temperatures included in Figs. 10 and 11. At the higher temperatures there is merely a growing in of the inhomogeneous background, the evolution of the sharp lines themselves is identical to the one at 1.4 K. This is to be expected, as in the concentrated systems, the homogeneous line width as the crucial parameter does not vary much within this temperature interval. However, at 4.2 K the phonon-assisted process becomes dominant, all narrowed features being lost after 500 μs following the excitation. For $[Rh(bpy)_3][NaCr(ox)_3]ClO_4$, the hopping rate for the phonon-assisted process at 4.2 K can be estimated from the time-resolved spectra in Fig. 10. In the spectrum at a delay of ~100 μs the integrated intensity of the phonon-assisted background is almost identical to the integrated intensity of the sharp features, and therefore the hopping rate must also be of the order of $k_{et}^{ph} \approx 10^4\ s^{-1}$ at this temperature. Due to the higher density of low frequency phonons as compared to ruby and the somewhat larger ground state ZFS, phonon-assisted processes set in a lower temperature in the oxalate networks.

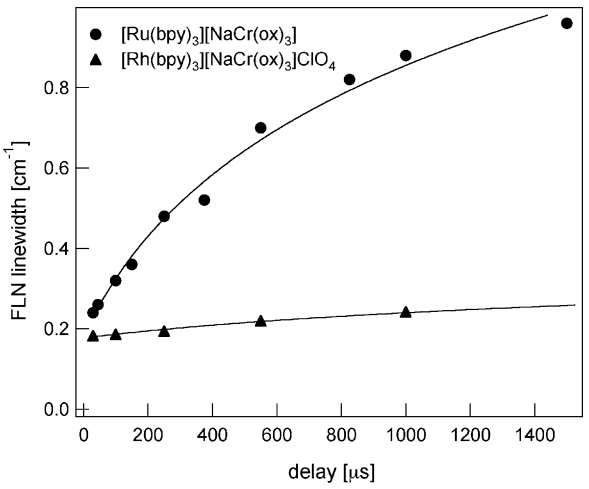

Fig. 13. Evolution of the line width as a function of delay time for of the sharp lines in the FLN spectra at 1.4 K of $[Rh(bpy)_3][NaCr(ox)_3]ClO_4$ (▲) and $[Ru(bpy)_3][NaCr(ox)_3]$ (●).

5. Conclusions

The very specific crystal structure of the model compounds with a strictly alternating sequence of sodium and chromium ions in the oxalate backbone ensures that exchange interactions between chromium ions are negligible, and that therefore the interaction between the chromophores is restricted to multipole–multipole interactions. As a result, three different mechanisms of non-radiative energy migration within the electronic origin of the $R_1(^4A_2 \rightarrow {}^2E)$ transition of $[Cr(ox)]^{3-}$ could be identified in the three-dimensional network compound. In addition to the common energy non-selective phonon-assisted process, previously observed in a number Cr^{3+} doped oxides, two different resonant and thus energy selective processes can be observed down to 1.4 K. The first one occurs between different ground state components. It is dominant if the inhomogeneous line width is substantially larger than the ground state ZFS, and it gives rise to a multi-line pattern in FLN spectra with spacings equal to the ground state ZFS of $D = 1.3\ cm^{-1}$. The second one occurs between the same components of the ground state and in an FLN spectrum gives rise to spectral diffusion of the initially sharp lines. It is dominant for small inhomogeneous distributions, which result in a higher concentration of species resonant within one homogeneous line width.

Whereas the inhomogeneous line width as well as the ground state ZFS are comparatively easy to determine experimentally, the third crucial parameter, the homogeneous line width is much more

difficult to determine. The value obtained in the steady state transient hole-burning experiment does not necessarily correspond to the correct value as it might already show some broadening through energy migration and power broadening. Even though in the discussion equal values for the homogeneous line width in the systems were assumed, this is by no means certain and will have to be ascertained. Both problems can and will be addressed with time-resolved hole-burning.

The surprisingly large value of R_c for Förster-type energy transfer is due to the small homogeneous line width of the purely electronic transition at low temperatures, which counteracts the small oscillator strength of the formally symmetry and spin-forbidden transition. In $[Rh(bpy)_3][NaCr(ox)_3]ClO_4$, the resonant energy migration goes on average over at least 5 steps down the ladder and probably also over an equal number of quasi-resonant steps. At more than 20 Å per step, the energy migrates up to 200 Å on average. As mentioned above, in $[Ru(bpy)_3][NaCr(ox)_3]$ the resonant or quasi-resonant process is as much as 10 times faster, and therefore the energy could migrate up to 2000 Å. In contrast, phonon-assisted migration is a hopping process between nearest neighbours and thus is limited to 9.4 Å only per step.

Finally, the effect of applying an external magnetic field could give some further insight into the role of the homogeneous line width for the resonant energy transfer process, because an external magnetic field reduces the electron-spin–electron-spin relaxation and thus the homogeneous line width substantially. Another intriguing question to ask and indeed to be addressed is, is it possible to burn persistent side-holes via resonant energy transfer in a system, which shows persistent hole burning such as the $NaMg[Al(ox)_3]x9H_2O$ system studied by Riesen and Hughes [48] and the step-wise energy migration of the oxalate networks simultaneously.

Acknowledgement

We thank the Swiss National Science Foundation for financial support of this work.

References

[1] Advanced solid state lasers, in: M.M. Fejer, H. Injeyan, U. Keller (Eds.), in: OSA Trends in Optics and Photonics, vol. 26, Optical Society of America, Washington, 1999.
[2] T. Justel, H. Nikol, C. Ronda, Angew. Chem. Int. Ed. 37 (1998) 3084.
[3] M. Grätzel, Nature 414 (2001) 338.
[4] (a) R.M. Clegg (Ed.), Rev. Mol. Biotechnol. 82 (2002) 177;
(b) D.L. Andrews, A.A. Demidov (Eds.), Resonance Energy Transfer, Wiley, Chichester, 1999.
[5] (a) G. Blasse, K.C. Powell, Structure and Bonding, vol. 42, Springer, Heidelberg, 1980;
(b) B. DiBartolo (Ed.), Energy Transfer Processes in Condensed Matter, NATO ASI Series B, vol. 114, Plenum, New York, 1985;
(c) B. DiBartolo, X. Chen (Eds.), Advances in Energy Transfer Processes, World Scientific, New Jersey, 2001.
[6] B. Henderson, G.F. Imbusch, Optical Spectroscopy of Inorganic Solids, Clarendon Press, Oxford, 1989.
[7] (a) F. Auzel, G. Baldacchini, J. Lumin. 125 (2007) 25;
(b) F. Auzel, F. Bonfigli, S. Gagliari, G. Baldacchini, J. Lumin. 94–95 (2001) 293.
[8] M. Hehlen, J. Opt. Soc. Am. B 14 (1997) 1312.
[9] T. Förster, Ann. Phys. 2 (1948) 55.
[10] D.L. Dexter, J. Chem. Phys. 21 (1953) 836.
[11] C.B. Harris, D.A. Zwemer, Ann. Rev. Phys. Chem. 29 (1978) 473.
[12] (a) T. Holstein, S.K. Lyo, R. Orbach, Phys. Rev. Lett. 36 (1976) 891;
(b) T. Holstein, S.K. Lyo, R. Orbach, in: W.M. Yen, P.M. Selzer (Eds.), "Laser Spectroscopy of Solids", Topics in Applied Physics, vol. 49, Springer, Berlin, 1981, p. 39.
[13] (a) S. Xia, P.A. Tanner, Phys. Rev. B 66 (2002) 214305;
(b) P.A. Tanner, in: H. Yersin (Ed.), Topics in Current Chemistry, vol. 241, Springer, Berlin, 2004, p. 167.
[14] G.F. Imbusch, W.H. Yen, in: W.M. Yen, M.D. Levenson (Eds.), Lasers, Spectroscopy and New Ideas, Optical Series, vol. 54, Springer, Berlin, 1987, p. 248.
[15] (a) A. Hauser, M.E. von Arx, V.S. Langford, S. Kairouani, U. Oetliker, A. Pillonnet, in: H. Yersin (Ed.), Topics in Current Chemistry, vol. 241, Springer, Berlin, 2004, p. 65;
(b) M.E. von Arx, V.S. Langford, U. Oetliker, A. Hauser, J. Phys. Chem. A 106 (2002) 7099;
(c) M.E. von Arx, A. Hauser, H. Riesen, R. Pellaux, S. Decurtins, Phys. Rev. B54 (1996) 15800.
[16] S. Sugano, Y. Tanabe, H. Kamimura, Pure and Applied Physics, vol. 33, Academic Press, New York, 1970.
[17] (a) A.W. Adamson, W.L. Waltz, E. Zinato, D.W. Watts, P.D. Fleischauer, R.D. Lindholm, Chem. Rev. 68 (1968) 541;
(b) A.W. Adamson, Coord. Chem. Rev. 3 (1968) 169;
(c) G. Irwin, A.D. Kirk, Coord. Chem. Rev. 211 (2001) 25;
(d) E. Zinato, P. Riccieri, Coord. Chem. Rev. 211 (2001) 5;
(e) A. Derwahl, F. Wasgestian, D.A. House, W.T. Robinson, Coord. Chem. Rev. 211 (2001) 45.
[18] L.S. Forster, Coord. Chem. Rev. 248 (2004) 261.
[19] L.E. Collins, M.A. Morrison, P.L. Donoho, Am. J. Phys. 42 (1974) 560.
[20] A. Szabo, Phys. Rev. Lett. 25 (1970) 924.
[21] P.M. Selzer, in: W.M. Yen, P.M. Selzer (Eds.), "Laser Spectroscopy of Solids", Topics in Applied Physics, vol. 49, Springer, Berlin, 1981, p. 113.
[22] W.M. Yen, P.M. Selzer, in: W.M. Yen, P.M. Selzer (Eds.), "Laser Spectroscopy of Solids", Topics in Applied Physics, vol. 49, Springer, Berlin, 1981, p. 141.
[23] (a) A. Szabo, Phys. Rev. B 11 (1975) 4512;
(b) T. Muramoto, S. Nakamishi, T. Hashi, Opt. Commun. 21 (1977) 139.
[24] S. Decurtins, H.W. Schmalle, R. Pellaux, P. Schneuwly, A. Hauser, Inorg. Chem. 35 (1996) 1451.
[25] (a) S. Decurtins, R. Pellaux, Comments Inorg. Chem. 20 (1998) 143;
(b) S. Decurtins, R. Pellaux, G. Antorrena, F. Pallacio, Coord. Chem. Rev. 192 (1999) 841;
(c) E. Coronado, J.R. Galan-Mascaros, C.J. Gomez-Garcia, J.M. Martinez-Agudo, Inorg. Chem. 40 (2001) 113.
[26] (a) T. Schönherr, J. Spanier, H.H. Schmidtke, J. Phys. Chem. 93 (1989) 5969;
(b) O.S. Mortensen, J. Chem. Phys. 47 (1969) 4215.
[27] T. Brunold, H.U. Güdel, in: E.I. Solomon, A.B.P. Lever (Eds.), Inorganic Electronic Structures and Spectroscopy, vol. 1, Wiley, New York, 1999.
[28] S. Lahity, R. Kakkar, Chem. Phys. Lett. 88 (1982) 499.
[29] M.L. Lewis, H. Riesen, J. Phys. Chem. A 106 (2002) 8039.
[30] (a) L.S. Forster, Coord. Chem. Rev. 227 (2002) 59;
(b) M. Yamaga, B. Henderson, K.P. O'Donnell, J. Phys.: Condens. Matter 1 (1989) 9175;
(c) N.J. Linck, S.J. Berens, D. Madge, R.G. Linck, J. Phys. Chem. 87 (1983) 1733.
[31] (a) H. Riesen, Struct. Bond. 107 (2004) 179;
(b) H. Riesen, Coord. Chem. Rev. 250 (2006) 1737.
[32] (a) J.L. Hughes, H. Riesen, J. Phys. Chem. A 107 (2003) 35;
(b) H. Riesen, J.L. Hughes, Chem. Phys. Lett. 370 (2003) 26.
[33] C.A. Bates, J.P. Bentley, R.A. Lees, W.S. Moore, J. Phys. C 2 (1969) 1970.
[34] (a) L.M. Lewis, H. Riesen, PCCP 4 (2002) 4845;
(b) H. Riesen, E. Krausz, J. Chem. Phys. 97 (1992) 7902.
[35] G.F. Imbusch, W.M. Yen, A.L. Schawlow, D.E. McCumber, M.D. Sturge, Phys. Rev. 133 (1964) A1029.
[36] C. Ecolivet, S. Rabaste, A. Hauser, Results from Brillouin scattering, unpublished.
[37] M. Lucht, M. Lerche, H.-C. Wille, Yu.V. Shvyd'ko, H.D. Rüter, E. Gerdau, P. Becker, J. Appl. Cryst. 36 (2003) 1075.
[38] J.R. Lakowicz, Principles of Fluorescence Spectroscopy, 3rd ed., Springer, Berlin, 2006.
[39] S.A. Basun, R.S. Meltzer, G.F. Imbusch, J. Lumin. 125 (2007) 31.
[40] G.F. Imbusch, Phys. Rev. 153 (1967) 326.
[41] (a) P.M. Selzer, D.S. Hamilton, W.M. Yen, Phys. Rev. Lett. 38 (1977) 858;
(b) P.M. Selzer, D. L-Huber, B.B. Barnett, W.M. Yen, Phys. Rev. B. 17 (1978) 4979.
[42] A. Monteil, E. Duval, J. Phys. C 12 (1979) L416.
[43] P.E. Jessop, A. Szabo, Phys. Rev. Lett. 45 (1980) 1712.
[44] S. Chu, H.M. Gibbs, S.L. Call, A. Passner, Phys. Rev. Lett. 45 (1980) 1715.
[45] Z. Hasan, S.T. Keany, N.B. Manson, J. Phys. C 19 (1986) 6381.
[46] (a) P.M. Selzer, D.S. Hamilton, R. Flach, W.M. Yen, J. Lumin. 12–13 (1976) 737;
(b) P. Avouris, A. Campion, M.A. El-Sayed, Chem. Phys. Lett. 50 (1977) 9;
(c) I.Y. Chan, B.L. Goldenberg, J. Chem. Phys. 79 (1983) 3711;
(d) R. Balda, J. Fernandez, J.L. Adam, M.A. Arriandiaga, Phys. Rev. B 54 (1996) 12076.
[47] M. Inokuti, F. Hirayama, J. Chem. Phys. 43 (19651978).
[48] H. Riesen, J.L. Hughes, Chem. Phys. Lett. 372 (2003) 563.